CHARACTERIZATION AND MEASUREMENT OF DISPERSIVE CHANNELS

J. L. Ramsey

NOVEMBER 1971

Prepared for

DEPUTY FOR PLANNING AND TECHNOLOGY
ELECTRONIC SYSTEMS DIVISION
AIR FORCE SYSTEMS COMMAND
UNITED STATES AIR FORCE
L. G. Hanscom Field, Bedford, Massachusetts

Project 511A

Prepared by

THE MITRE CORPORATION
Bedford, Massachusetts

Contract F19(628)-71-C-0002

ESD-TR-71-382

MTR-2184

CHARACTERIZATION AND MEASUREMENT OF DISPERSIVE CHANNELS

J. L. Ramsey

NOVEMBER 1971

Prepared for

DEPUTY FOR PLANNING AND TECHNOLOGY
ELECTRONIC SYSTEMS DIVISION
AIR FORCE SYSTEMS COMMAND
UNITED STATES AIR FORCE
L. G. Hanscom Field, Bedford, Massachusetts

Project 511A

Prepared by

THE MITRE CORPORATION
Bedford, Massachusetts

Contract F19(628)-71-C-0002

FOREWORD

This report has been prepared by The MITRE Corporation under Project 511A of Contract F19(628)-71-C-0002. The contract is sponsored by the Electronic Systems Division, Air Force Systems Command, L. G. Hanscom Field, Bedford, Massachusetts.

REVIEW AND APPROVAL

Publication of this technical report does not constitute Air Force approval of the report's findings or conclusions. It is published only for the exchange and stimulation of ideas.

KENNETH H. KRONLUND
Lt Colonel, USAF
CNI/PLRACTA Program Manager
Directorate of Communications Systems Planning

ABSTRACT

This report is concerned with the characterization and study of dispersive channels. It shows how and why the physical channel distorts signals, it presents an experimental program for acquiring data to characterize the channel, and it indicates how the experimental data could be used either to evaluate the performance of arbitrary signaling techniques or to design effective signals for communicating over the channel.

ACKNOWLEDGMENTS

The author wishes to thank M. R. Dresp and D. K. Leichtman of MITRE and P.A. Bello and H. Salwen of SIGNATRON, Inc., for a number of useful comments and suggestions that have been incorporated throughout the text, especially in Sections IV and V.

TABLE OF CONTENTS

TABLE OF CONTENTS (cont.)

LIST OF ILLUSTRATIONS

SECTION I

INTRODUCTION

1.1 The Communication Problem

Almost all electrical signals that are used to represent a message are corrupted, apart from being attenuated, in their passage through the transmission medium from sender to receiver. If this were not so, there would be little need for the services of communication systems engineers; it would be relatively easy to design noiseless, distortionless amplifiers to amplify the attenuated but otherwise undistorted signal to its original level, and thus to reproduce exactly the transmitted message. Indeed, it is the need to overcome the effects of the random, unknown pertubations that corrupt the received signal that engenders the study of communication over corruptive transmission media.

1.2 Sources of Signal Corruption

Signals transmitted over some appropriate medium can be corrupted in two general ways. The first way is that some unwanted and unknown signal, called noise, is added to the received waveform. There are many sources of this unwanted noise, ranging from thermal "front end" noise in the receiver, atmospheric noise, unintentional electrical noise produced by extraneous electrical devices, unintentional interference produced by other transmitters, and intentional interference produced by jammers. To some extent the problem of detecting signals transmitted in additive noise has been extensively studied, especially in the case of thermal noise [1]. Since the additive noise is produced independently of the transmitted signal, the ratio of received signal energy to noise energy increases indefinitely as the signal power is increased. Thus for additive noise channels the performance of a communication system can be improved arbitrarily if the transmitted

signal power can be made sufficiently great. Of course, this may be an inefficient technique for achieving reliable communications.

A second, more insidious form of signal corruption is caused by signal dispersion, whereby the signal travels two or more distinct paths from the transmitter to the receiver. This form of corruption is sometimes called "the multipath problem"; one common example is the presence of "ghosts" on a television receiver. If the transmission paths do not all have the same length, then the received signal consists of a summation of successively delayed and phase-shifted versions of the transmitted signal. Even when the difference in transmission times among the various paths is much less than the duration of the transmitted signal, the received signal can be severely distorted -- perhaps unrecognizable. This form of signal corruption cannot be overcome merely by increasing the transmitter power, since the contribution from each reflected path is also increased accordingly.

1.3 Scope and Objectives of this Report

The remainder of this report is concerned only with the characterization and study of dispersive channels. We show how and why the physical channel distorts signals, we present an experimental program to measure the dispersive parameters of the channel, and we show how to use the data obtained from the experimental program both to evaluate the performance of arbitrary signaling techniques, and to design effective signals for communicating over the channel. Section II derives three alternative ways of mathematically expressing the channel output in terms of the input and the physical scattering mechanism of the channel. Section III shows how time- and frequency-dispersive channels distort signals by producing frequency- and time-selective fading. Section IV describes an experimental channel measurements program that could be used both to design and to evaluate signaling techniques. Section V shows how the experimental data could be used to evaluate the performance of arbitrary but bandlimited signals,

while Section VI indicates some of the considerations involved in using the experimental data to design effective signaling techniques.

1.4 Complex Notation

In this report, we employ complex notation to represent narrowband real signals. If the transmitted signal is

$$s(t) = \mathrm{Re}\{x(t)\, e^{j2\pi f_o t}\}, \tag{1}$$

then $x(t)$ is a narrowband, complex quantity called the complex envelope of $s(t)$, and f_o is a carrier frequency. The complex spectrum of $x(t)$ is the Fourier transform

$$X(f) = \int x(t)\, e^{-j2\pi ft}\, dt. \tag{2}$$

By "narrowband", we mean that

$$|X(f)| = 0, \quad f \geq F, \; F \ll f_o. \tag{3}$$

SECTION II

DETERMINISTIC MODELS OF A DISPERSIVE CHANNEL

We now present three equivalent mathematical representations of the scattering produced by a linear dispersive radio channel. Our formulations are taken from Daly [2] and Kennedy [3].

2.1 Time-Variant Narrowband Transfer Function

A linear multipath channel can conceptually be regarded as being composed of a (perhaps very large) collection of discrete paths or scatterers. Let the input to the channel be

$$s(t) = \mathrm{Re}\{e^{j2\pi(f_o+f)t}\}, \quad o \leq |f| << f_o, \tag{4}$$

a unit sinusoid at frequency f_o+f. The signal received by having been reflected from the k^{th} scatterer has the form

$$r_k(t) = \mathrm{Re}\{a_k e^{j2\pi(f_o+f+\lambda_k)(t-\tau_k)}\} \tag{5}$$

where λ_k is a Doppler shift, τ_k is a time delay, and a_k is a complex multiplier representing the magnitude (cross section) and phase shift of the reflection from the k^{th} scatterer. Equation (5) can be re-written as

$$r_k(t) = \mathrm{Re}\left\{\left[b_k e^{j2\pi\lambda_k t} e^{-j2\pi\tau_k f}\right] e^{j2\pi(f_o+f)t}\right\} \tag{6}$$

where

$$b_k = a_k e^{-j2\pi\tau_k(f_o+\lambda_k)}. \tag{7}$$

Consider the output $r(t)$ of the linear multipath channel due to the unit sinusoidal input (4) which, in the absence of noise, is the sum of the

reflected signals from each of the discrete scatterers. Let y(t) be the complex envelope of r(t) with respect to the carrier frequency f_o. If we define

$$H(t,f) = \sum_k b_k \, e^{j2\pi\lambda_k t} \, e^{-j2\pi\tau_k f} \tag{8}$$

then be summing and using (8) we obtain

$$\begin{aligned} r(t) &= \sum_k r_k(t) \\ &= \text{Re}\left\{e^{j2\pi(f_o+f)t} \sum_k b_k e^{j2\pi\lambda_k t} e^{-j2\pi\tau_k f}\right\} \\ &= \text{Re}\left\{H(t,f)\, e^{j2\pi(f_o+f)t}\right\} \\ &= \text{Re}\left\{y(t)\, e^{j2\pi f_o t}\right\} \end{aligned} \tag{9}$$

By comparing (9) and (1) we observe that H(t,f) is the complex envelope of the channel response to a unit sinusoid at frequency f_o+f. Thus we have the following physically intuitive interpretation: H(t,f) can be regarded as the time-variant narrowband transfer function of a linear multipath channel.

Since the channel is linear, the complex envelope of the channel output for a general input signal given by (1) or (2) is

$$y(t) = \int X(f)H(t,f)\, e^{j2\pi ft}\, df. \tag{10}$$

In Section 3.2 of this report we shall use the representation (8) to illustrate the presence and physical origin of time- and frequency-selective fading that occurs on a linear multipath channel. Before that, however, we derive two more equivalent representations of the channel behavior.

2.2 Time-Variant Impulse Response

An alternative representation can be derived to express the complex envelope of the channel output in terms of the complex envelope of the channel input rather than in terms of the complex spectrum of the channel input. Substituting (8) into (10) and using the inverse transform corresponding to (2), we obtain

$$y(t) = \sum_k b_k \; x\,(t-\tau_k)\; e^{j2\pi\lambda_k t}. \tag{11}$$

Equation (11) was derived strictly as a mathematical operation on X(f) and H(t,f). It can, however, be easily derived from physical reasoning as well. Equation (11) merely states that the output of a linear multipath channel consisting of a collection of discrete scatterers is the sum of the reflections from each scatterer, where τ_k is the delay of the k^{th} scatterer, λ_k is its Doppler shift, and b_k is the complex amplitude (amplitude and phase) of the k^{th} scatterer.

We are now ready to define the time-variant impulse response of the channel. As with linear time-invariant system theory, the time-variant impulse response should be the Fourier transform of the time-variant transfer function:

$$\begin{aligned} h(t,\tau) &= \int H(t,f)\; e^{j2\pi f\tau} df \\ &= \sum_k b_k\; \delta\,(\tau-\tau_k)\; e^{j2\pi\lambda_k t}, \end{aligned} \tag{12}$$

where $\delta(x)$ is a delta function. To show that $h(t,\tau)$ is indeed the time-variant impulse response of the channel, it suffices to show that for any input whose complex envelope is x(t), the complex envelope of the output reduces to Equation (11):

$$y(t) = \int x\ (t-\tau)\ h\ (t,\tau)\ d\tau$$

$$= \int \sum_k b_k\ x\ (t-\tau)\ \delta\ (\tau-\tau_k)\ e^{j2\pi\lambda_k t}\ d\tau$$

$$= \sum_k b_k\ x\ (t-\tau_k)\ e^{j2\pi\lambda_k t}. \qquad (13)$$

It is intuitively satisfying that $H(t,f)$ and $h(t,\tau)$ are Fourier transform pairs. Physically, $h(t,\tau)$ can be interpreted as the complex envelope of the channel response at time t due to a unit impulse applied at time $t-\tau$.

2.3 Delay-Line Model

We now present a third way of modeling the behavior of a linear time-variant channel. This model is especially well suited to suggesting an experimental technique whereby the exact performance of an experimental channel can be recorded and later used in a playback device to evaluate and simulate behavior of any suitably bandlimited signal that might be applied to the channel. The details of this measurement and evaluation technique will be presented in Sections IV and V.

Suppose, as in (3), we restrict our attention to bandlimited signals whose bandwidth is narrow with respect to the carrier frequency. Suppose also that without loss of generality the minimum scatterer delay is zero, and that the maximum delay is τ_M. We now invoke the fact that a waveform of bandwidth 2F does not change its value appreciably in time intervals $\Delta t_F << \frac{1}{2F}$. More explicitly, this means that

$$x(t) \cong x(t-\tau) \text{ for all } |\tau| \leq \Delta t_F. \qquad (14)$$

We now divide the time interval $[0,\tau_M]$ into

$$N_F = \frac{\tau_M}{\Delta t_F} + 1 \tag{15}$$

subintervals of length Δt_F, and we say that

$$\tau_k \in T_j \tag{16}$$

if

$$(j-1)\Delta t_F \leq \tau_k < j\Delta t_F, \; j = 1, 2, \ldots, N_F. \tag{17}$$

Then we can rewrite (11) as a tapped delay-line model:

$$y(t) \cong \sum_{j=1}^{N_F} m_j(t) \; x \left[t - (j-1)\Delta t_F\right] \tag{18}$$

where

$$m_j(t) = \sum_{k:\tau_k \in T_j} b_k \, e^{j2\pi\lambda_k t} \tag{19}$$

is the complex gain function of the j^{th} tap. Explicitly, the complex envelope of the channel output is equal to the summation of N_F complex waveforms, each of which is equal to the product of the complex envelope of the channel input, suitably delayed, and a complex tap gain function.

Observe that if the Doppler shifts are bounded by

$$|\lambda_k| \leq \lambda \text{ for all } k, \tag{20}$$

then by applying the Nyquist Theorem we find that the bandwidth of each of the tap gain functions is no greater than 2λ.

SECTION III

SELECTIVE FADING CHANNELS

3.1 Dispersion

Strictly speaking, any multipath channel consisting of two or more distinct, resolvable paths is dispersive, since the signals received from the different paths either do not all arrive at the receiver at the same time or the Doppler shifts of the paths are not all the same or both. A channel is said to be time-dispersive if the delays of each of the scatterers are not identical, and it is frequency-dispersive if the Doppler shifts of each of the scatterers are not identical. Revising Kennedy's[3] definitions somewhat, we say that a channel is slightly time-dispersive if the maximum spread in the scatterer delays is small compared to the time intervals of interest that describe the signal structure, and similarly it is slightly frequency-dispersive if the maximum spread in the scatterer Doppler shifts is small compared to the signal bandwidths. As we shall see later, even slightly dispersive channels can introduce significant signal distortion.

We now develop quantitative expressions that define the time- and frequency-dispersion of a channel. Recall that each resolvable discrete scatterer is characterized by a magnitude and phase shift, a time delay, and a Doppler shift. For the unit sinusoidal input (4), the amount of power that is reflected with a delay of τ_k and a Doppler shift λ_k is

$$\sigma_k^2 = |b_k|^2. \tag{21}$$

We define the channel scattering function $S(\lambda,\tau)$ to be the two-dimensional power density of power scattered by the channel as a function of Doppler shift λ and time delay τ. For our representation of the channel,

$$S(\lambda,\tau) = \sum_k \sigma_k^2 \, \delta(\lambda-\lambda_k) \, \delta(\tau-\tau_k). \tag{22}$$

The total power scattered by the channel is

$$P = \iint S(\lambda,\tau) \, d\lambda \, d\tau. \tag{23}$$

The marginal densities of power scattered by the channel as a function of Doppler shift only or time delay only are called, respectively[2], the Doppler profile $D(\lambda)$ and the time-delay profile $T(\tau)$. Thus

$$D(\lambda) = \int S(\lambda,\tau) \, d\tau \tag{24}$$

and

$$T(\tau) = \int S(\lambda,\tau) \, d\lambda \, . \tag{25}$$

The time- and frequency-dispersion of a channel can be quantatively expressed in terms of the time-delay spread σ_τ and the Doppler spread σ_λ, which are the square roots of the normalized second moments of $T(\tau)$ and $D(\lambda)$ respectively[2]:

$$\sigma_\tau^2 = \frac{1}{P} \int \tau^2 T(\tau) \, d\tau, \tag{26}$$

and

$$\sigma_\lambda^2 = \frac{1}{P} \int \lambda^2 \, D(\lambda) \, d\lambda. \tag{27}$$

These spreads indicate the extent to which the channel spreads power in the time and frequency domains.

3.2 Selective Fading

We will now show how dispersive channels produce selective fading. A channel is said to exhibit frequency-selective fading if at any given time the fading -- i.e., the channel gain and phase shift -- is not identical for all frequencies within the channel bandwidth. Similarly, a channel exhibits time-selective fading if the fading on any given frequency varies with time. As we will presently see, frequency-selective fading is caused by time dispersion within the channel, and time-selective fading is caused by frequency dispersion.

Consider the time-variant transfer function (8). At any given time t',

$$H(t',f) = \sum_k c_k \, e^{-j2\pi\tau_k f}, \tag{28}$$

where

$$c_k = b_k e^{j2\pi\lambda_k t'}. \tag{29}$$

If $\sigma_\tau = 0$ -- i.e., if all of the $\{\tau_k\}$ are identical -- then the fading will be identical on all frequencies. Otherwise the complex envelope varies with frequency, indicating the presence of frequency-selective fading which is caused by the time delays $\{\tau_k\}$.

Similarly at any given frequency f',

$$H(t,f') = \sum_k d_k \, e^{j2\pi\lambda_k t}, \tag{30}$$

where

$$d_k = b_k \, e^{-j2\pi\tau_k f'}. \tag{31}$$

If $\sigma_\lambda = 0$ the fading will be time invariant. Otherwise the complex envelope varies with time, indicating the presence of time-selective fading which is caused by the Doppler shifts $\{\lambda_k\}$.

The degree of time- and frequency-selective fading exhibited by a dispersive channel can be quantitatively expressed in terms of the coherence time T_c and coherence bandwidth (correlation bandwidth) B_c, respectively. These quantities are conveniently but arbitrarily related to a statistical characterization of the channel, which we shall discuss presently. We shall also observe that the coherence time and bandwidth are not independent of the time-delay and Doppler spreads previously defined, but that, as a rough rule of thumb, the coherence time is the reciprocal of the Doppler spread, and the coherence bandwidth is the reciprocal of the time-delay spread.

The coherence time and bandwidth have the physical interpretation that the channel fading is essentially independent between samples spaced in time by more than T_c seconds, and that the channel fading is essentially independent for two tones spaced by more than B_c Hz. Furthermore, the coherence time and bandwidth are useful parameters to guide in the design of signaling structures and demodulation techniques. For example, one cannot usefully employ coherent detection techniques if the signal duration greatly exceeds T_c.

To provide a suitable statistical characterization of the channel, we now make the assumption that the fading or reflections from different scatterers are physically and statistically independent, and that the phase of the reflection from each scatterer is uniformly distributed over the interval $[0,2\pi]$. These assumptions imply that the $\{b_k\}$ defined in (7) are zero-mean complex random variables for which

$$E(b_k^* b_j) = \begin{cases} \sigma_k^2, & j = k, \\ 0, & j \neq k, \end{cases} \tag{32}$$

where $E(\cdot)$ is the statistical expectation, and σ_k^2 is defined by (21).

We now define the time-frequency autocorrelation function of the channel as

$$R_H(\alpha,\beta) = \frac{1}{P} E\left[H^*(t,f)\ H\ (t+\alpha,\ f+\beta)\right]$$

$$= \frac{\sum_k \sigma_k^2\ e^{j2\pi\lambda_k\alpha}\ e^{-j2\pi\tau_k\beta}}{\sum_k \sigma_k^2}\ . \qquad (33)$$

Observe that $R_H(\alpha,\beta)$ is stationary in both t and f.

Using the preceding definition, we can now define the coherence time and coherence bandwidth of the channel. Observe that by applying (28) and (29) to (33), the normalized correlation of the envelopes of two unit sinusoids separated by β Hz is

$$R_H(\beta) = \frac{1}{P}\ E\left[H^*(t',f)\ H\ (t',\ f+\beta)\right]$$

$$= \frac{\sum_k \sigma_k^2\ e^{-j2\pi\tau_k\beta}}{\sum_k \sigma_k^2}\ . \qquad (34)$$

We define the coherence bandwidth B_c to be that value of β for which*

$$B_c = \inf_{\beta:\beta>0} \quad \text{for which Re}\{R_H(\beta)\} \leq 0.5 \qquad (35)$$

* There is nothing sacred about the value 0.5 used to define B_c in (35) or T_c in (37). Alternative values of 0 and $\frac{1}{e}$ have been used, all with more or less equal validity.

Similarly if

$$R_H(\alpha) = \frac{1}{P} E\left[H^*(t,f')\ H\ (t+\alpha,\ f')\right]$$

$$= \frac{\sum_k \sigma_k^2\ e^{j2\pi\lambda_k\alpha}}{\sum_k \sigma_k^2}\ , \qquad (36)$$

we define the coherence time T_c to be that value of α for which

$$T_c = \inf_{\alpha:\alpha>0} \text{ for which } \mathrm{Re}\ \{R_H(\alpha)\} \leq 0.5. \qquad (37)$$

We now heuristically justify our assertions that

$$T_c \cong \frac{1}{\sigma_\lambda} \qquad (38)$$

and

$$B_c \cong \frac{1}{\sigma_\tau}\ . \qquad (39)$$

To justify (38), observe from (36) that for $\alpha << \frac{1}{\sigma_\lambda}$, the product $\lambda_k\alpha$ is much less than unity for almost all k -- certainly for all k with significant σ_k -- so that the phase contributions to $R_H(\alpha)$ from strongly reflecting paths are essentially zero, and $\mathrm{Re}\ \{R_H(\alpha)\} > 0.5$. As α becomes greater than $\frac{1}{\sigma_\lambda}$, however, the phase contribution from each of the paths tends to become random with respect to the phase contributions from the other paths, and thus the condition (37) will be reached first for some α approximating (38). Equation (39) can be similarly justified.

3.3 Distortion

We have asserted earlier that even slightly dispersive channels can severely distort a signal transmitted through the channel. Clearly, channels which are not just slightly dispersive -- i.e., channels for which the time-delay spread is a significant fraction of the signal duration T, or for which the Doppler spread is a significant fraction of the signal bandwidth F, or both -- introduce noticeable distortion, since the received signals are discernably spread with respect to the transmitted signal in either or both the time or frequency domains. Even when $\sigma_\tau/T \ll 1$ and $\sigma_\lambda/F \ll 1$ there can be significant distortion, however, unless the conditions derived below are met.

We now derive the conditions for which the channel will not appreciably distort a signal, except for an attenuation and a phase shift. In the time domain we require that the significant reflected waveforms add coherently with respect to the complex envelope. This means that the time spread between significant reflections should be small compared to the time in which the complex envelope changes significantly. Using the fact that a waveform does not vary appreciably in intervals much less than the reciprocal of its bandwidth, one condition for distortionless transmission is that

$$\sigma_\tau F \ll 1. \tag{40}$$

Similarly, we also require that

$$\sigma_\lambda T \ll 1. \tag{41}$$

If (40) and (41) are satisfied simultaneously, the received waveform will be an essentially undistored replica of the transmitted signal. Since the TF product for any waveform cannot be much less than 1, (40) and (41) imply that distortionless transmission is possible only for

those channels for which

$$\sigma_\tau \sigma_\lambda \ll 1. \tag{42}$$

The condition (42) is satisfied for many practical classes of dispersive channels, however.

SECTION IV

AN EXPERIMENTAL PROGRAM FOR MEASURING 10 MHz CHANNELS

In this section we describe an experimental program for acquiring data that can be used to design and to evaluate signals transmitted over a 10 MHz-bandlimited multipath channel.

4.1 Channel Characteristics to be Measured

A communication system designer can use the data from a propagation measurements experiment for two purposes: to help him design appropriate signaling structures for communicating over the channel, and to evaluate the performance of a given signaling technique. The channel characteristics that must be known are somewhat different for each of these objectives, however.

4.1.1 Channel Characteristics Required for Signal Design

A system designer should know the following characteristics of a multipath channel in order to properly design an effective communications signal:

a. Coherence bandwidth,

b. Coherence time;

c. Statistical characterization of fading as a function of time for a given frequency. This characterization should include as a minimum the distribution functions of the durations of fades and of the intervals between fades, for fades at various depths below the mean received signal level;

d. A similar statistical characterization of fading as a function of frequency for a given time;

e. A representative set of time-delay profiles. These profiles would provide various types of relevant information such as the interval between reception of the direct signal and the earliest reflected signal; a determination as to whether the scattering is specular, diffuse, or some combination; the ratio of the amplitude of the reflected signal to the amplitude of the direct signal; and the total interval over which significant signal energy is received.

He can then specify signaling techniques such as modulation, coding, diversity, and interleaving that are appropriate for effective communication over the channel.

4.1.2 Channel Characteristics Required for Signal Evaluation

As shown in Section 2.3, a tapped delay line model can always be used to represent the behavior the channel. If the complex, time-varying tap gains are known, it is possible to evaluate the channel response to an arbitrary input signal. The reciprocal of the temporal spacing between successive taps determines the maximum bandwidth of any input signal that can be evaluated; the number of taps determines the maximum time-delay (multipath) spread that can be tolerated for accurate evaluation; and the bandwidth of the recorded tap gain functions determines the maximum Doppler spread that can be accommodated.

4.1.3 Summary of the Experimental Measurements Program

A common channel probing signal can be used both to measure the characteristics of the channel relevant to signal design and to provide the set of complex, time-varying tap gain functions. The following propagation measurements program will accomplish both objectives:

1. Design a probing signal and construct suitable equipment for measuring and recording the channel characteristics that must be known for effective signal design.

2. Additionally, record the tap-gain data that can later be used directly as an input to a playback device to reproduce exactly the behavior of the probed channel.

4.2 Probing Signal and Transmitter Implementation

The channel probing signal consists of two elements. One element is a carrier that is phase modulated by a PN sequence produced by a maximal-length linear feedback shift register; the other element is a package of one or more phase-stable tones.

The chip length of the PN-modulated carrier must be no greater than half of the reciprocal of the bandwidth over which the channel can be characterized; this requires a chip length of no more than 1/20 μsec. to characterize a 10 MHz channel. If it is assumed that for some links there may be significant reflections which are delayed 100 μsec. from the direct path, the PN sequence should have a length of at least 2000 bits. A 12-tap linear feedback shift register generates a sequence whose length is 4095 bits, and this should be sufficient. Figure 1 is a block diagram showing the baseband equipment required to generate a suitable probing signal.

The only question that remains to be resolved is the number and spacing of the phase-stable tones. Several tones should be used in order to get a large sample of the temporal variations of fading. On the other hand, the correlation bandwidth of some media may be as great as 1 MHz, so that no more than 10 independent tones can be transmitted over a 10 MHz band. Finally the spectrum of the PN phase modulated carrier consists of a collection of discrete lines spaced over the RF band, with the spacing between adjacent lines being something like 5 kHz. Each of the phase-stable tones should be located as far as possible from the nearest spectral line, so that the received process corresponding to any stable tone can be passed

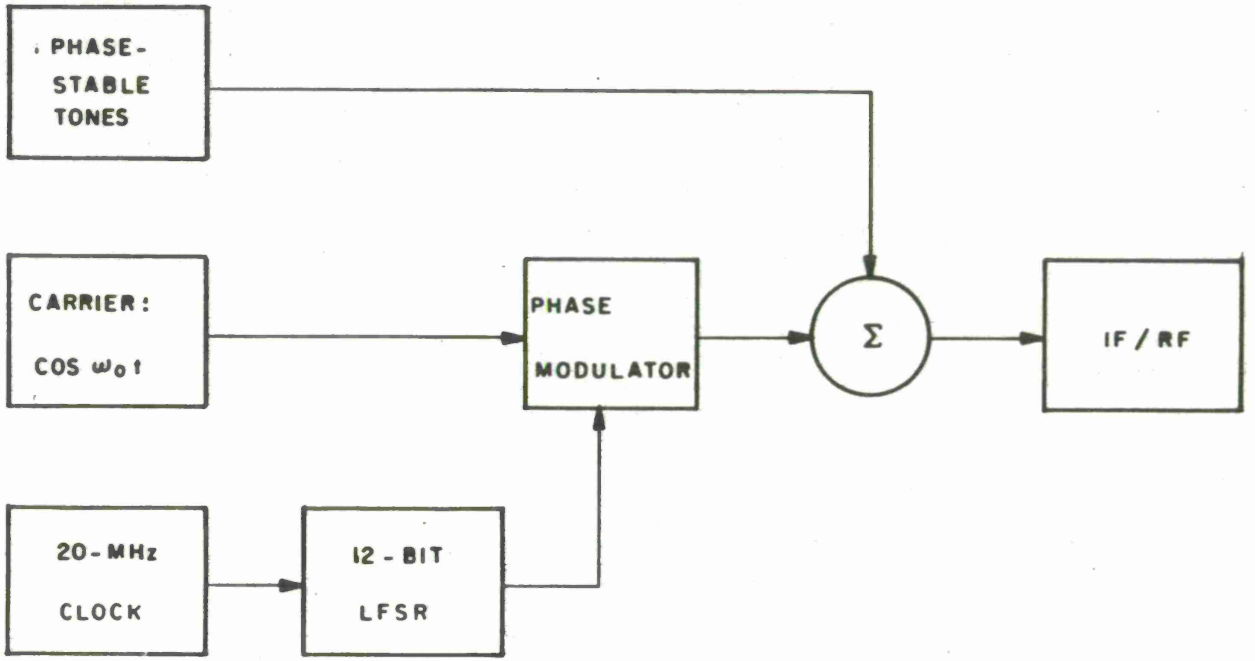

Figure 1. TRANSMITTER BLOCK DIAGRAM

through a narrowband filter to remove the effects of the remainder of the probing signal. With these considerations, the exact number and locations of phase-stable tones is a matter of engineering judgment that it is unnecessary to specify further at this time; a set of five tones spaced approximately 2 MHz apart would probably do nicely.

4.3 Signal Processing and Receiver Implementation

Figure 2 shows the block diagram of one realization of a base-band receiver structure of extracting the channel characteristics specified in Section 4.1. This receiver consists of a set of narrow-band filters tuned to each of the phase-stable tones, and a set of N tap-gain calculators which are used to calculate the complex time varying tap-gain functions that represent the scattering behavior of the channel. An AFC allows the receiver to track and compensate for any average Doppler shift introduced by relative motion between the transmitting and receiving terminals; its principal effect will be to minimize the bandwidth of the time-varying tap-gain functions, in order to minimize the sampling rate that must be used and recorded to characterize the channel.

The PN-modulated carrier is used to provide the time-delay profile and the records of fading as a function of frequency. The received PN signal is correlated with a succession of delayed in-phase and quadrature versions of the transmitted sequence; after filtering, these correlation functions become the complex tap-gain functions. These tap-gain functions are sampled at twice the filter bandwidths, and are recorded for later use in the optional playback device. The function corresponding to the magnitude (square root of the sum of the squares of the in-phase and quadrature components) of the tap gain functions represents the time-delay profile. The second central moment of the time-delay profile is the time-delay spread, and its reciprocal is approximately equal to the coherence bandwidth of the

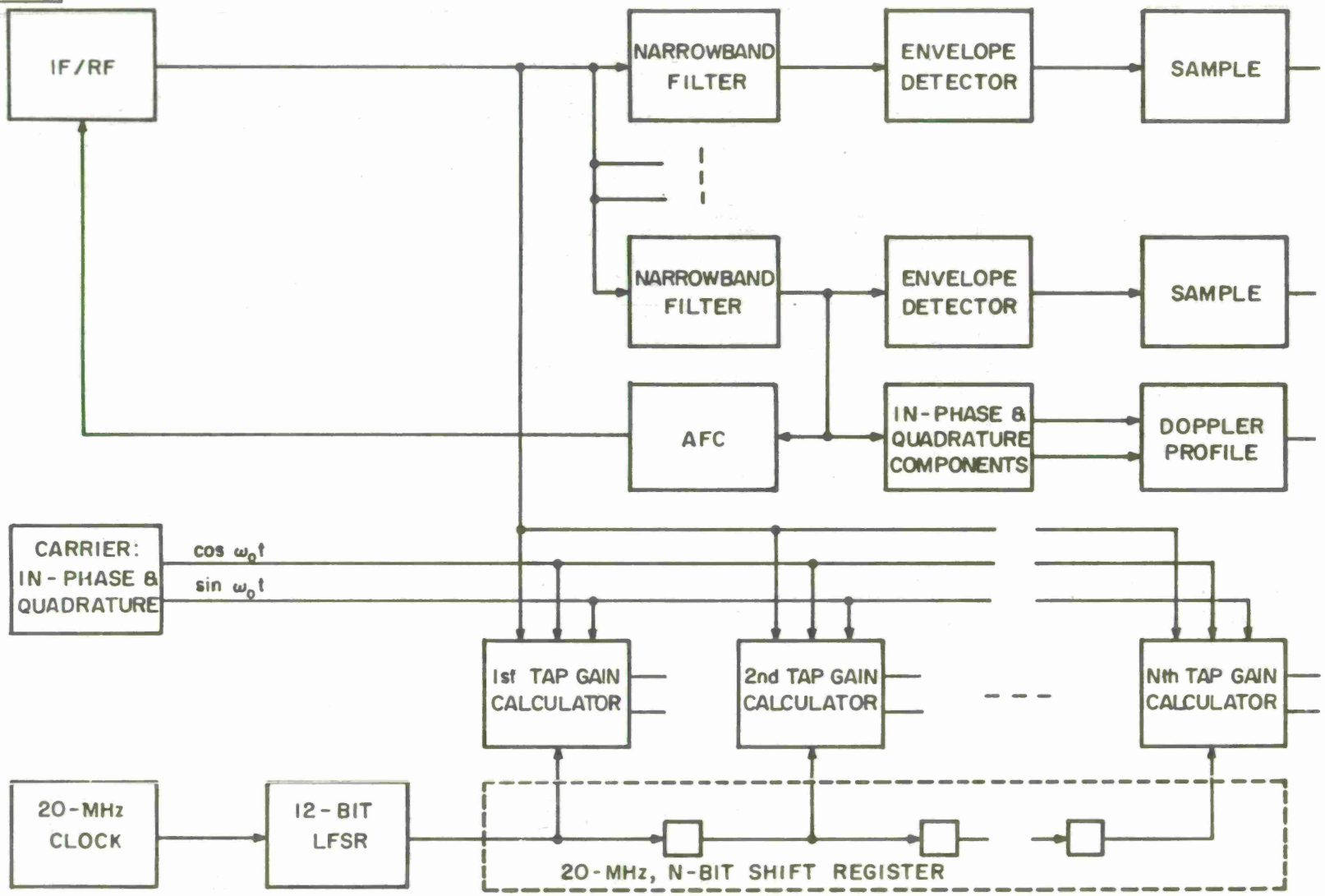

Figure 2 RECEIVER BLOCK DIAGRAM

channel. Whenever the PN sequence time of 200 μ sec. is much less than the channel coherence times to be expected, which is often the case, the tap-gain functions represent the complex time-varying impulse response at any given time. The Fourier transform of the time-varying impulse response is the time-varying transfer function observed at the same time, and the magnitude of this function provides a record of the fading as a function of frequency at the given time.

Figure 3 is a block diagram of the data processing in one of the tap-gain calculators. The basic outputs, $h_I(t, \tau_i)$ and $h_Q(t, \tau_i)$, are the measured values at time t of the in-phase and quadrature components of the complex time-variant impulse response of the channel evaluated at a delay τ_i from the time at which the direct (or earliest-arriving) component of the transmitted signal is received. If the largest differential Doppler shift between any multipath reflections is 200 Hz, for example, then the low-pass filters should be designed to cut off at 200 Hz, so that their outputs can be recovered from a 400 samples/sec. record. For a N-tap system with n-bit samples, the outputs can be recorded on n tracks of a multi-track tape recorder, provided it is capable of recording at least .8N kilobits/sec/track. These outputs can later be used directly as inputs to the playback device.

The question now arises as to how and when to compute and record the time-delay spreads and the records that indicate the variation of fading with frequency at periodic sampling times. One must consider the alternative possibilities of doing some preprocessing at the receiver and then recording, or of undertaking off-line calculations later. It may be more attractive to do preprocessing at the receiver, even though this option requires the use of a dedicated computer. For applications that do not require that samples of the spectral fading be taken more often than once per second, there are currently available high-speed computers (such as the CPS-30) that

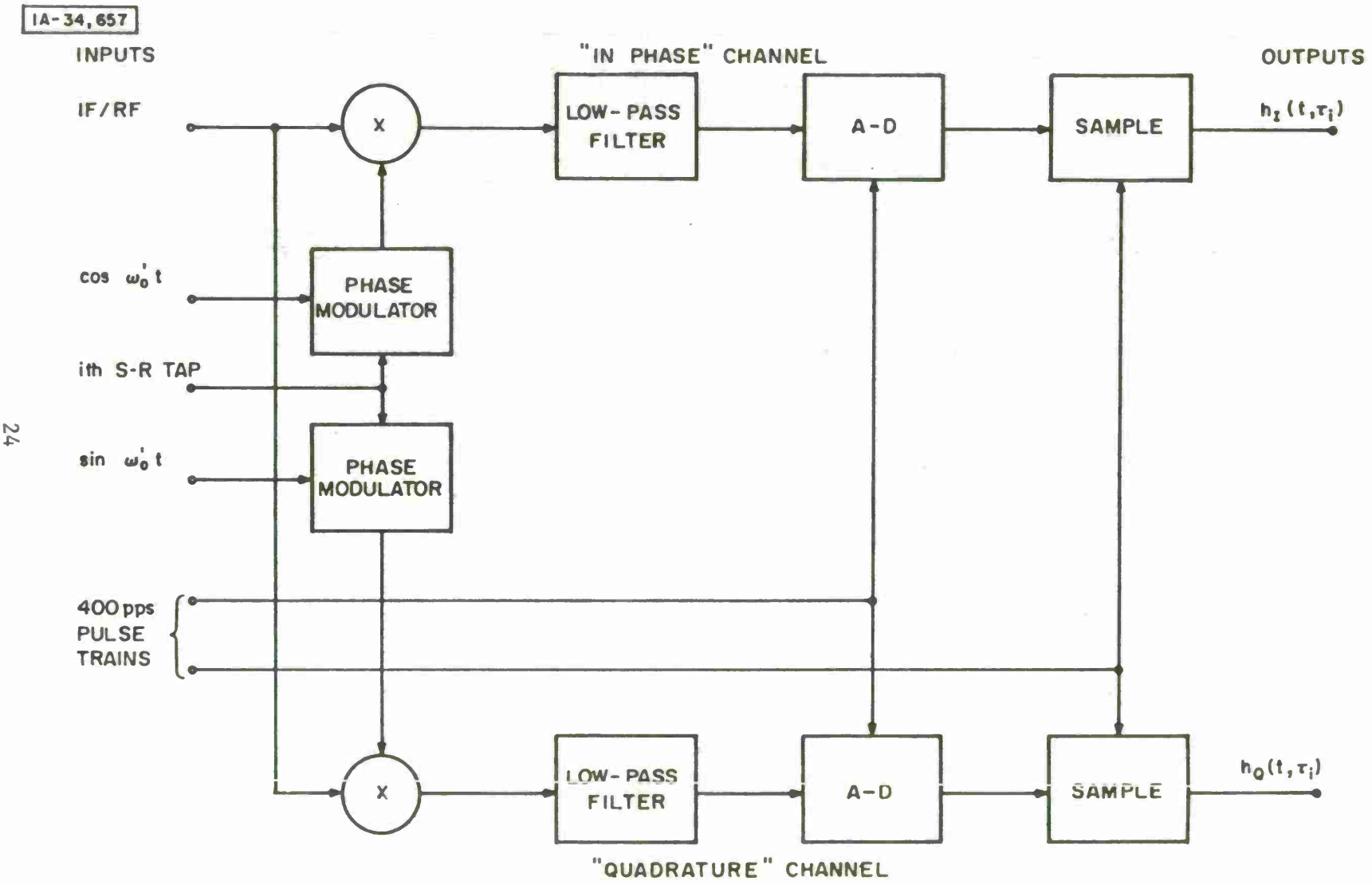

Figure 3 iTH TAP-GAIN CALCULATOR

are fast enough to process the data in real time. Each spectral fading record would be obtained as the Fourier transform of the time-variant impulse response of the channel sampled every second, which in turn corresponds to every 400^{th} set of complex tap-gain functions. The CPS-30 computer can perform a 4096 x 4096 complex FFT in about 190 ms -- leaving about 80% of its time free to undertake other calculations.

The phase-stable tones are used to provide the Doppler profile and the records of temporal fading. The Doppler profile can be extracted from one of the phase-stable tones in a manner similar to that described by Daly [4]: Long samples of the in-phase and quadrature components are recorded, and the Doppler profile can be calculated directly from these records by applying an appropriate FFT algorithm. The same computer used to calculate the records of spectral fading could also be used to calculate one Doppler profile per second, still leaving about 60% of the time for the computer to be available for other computations. The computer would then calculate the second central moment of the Doppler profile which is the Doppler spread, and its reciprocal is approximately equal to the coherence time of the channel.

A simpler alternative processing technique can be used to estimate just the Doppler spread. This technique arises from Rice's [5] observation that the average number of mean crossings per second, $\overline{N}_m$, of the envelope of a Gaussian random process is linearly related to the so-called "RMS bandwidth" of the process. For the received process corresponding to a transmitted phase-stable tone, the "RMS bandwidth" is equal to the Doppler spread of the communication channel. It can be shown [6] that for a linearly-detected envelope, assuming the received process is Gaussian,

$$N_m = 2.86\ \sigma_\lambda \tag{43}$$

It is relatively simple to build a device for measuring $\overline{N}_m$, in fact such a device was built by Stanford Research Institute in 1965 [6]. Figure 4 shows the accuracy of that device for two HF channels. Whether a comparable accuracy could be expected for high-bandwidth UHF, L-Band and higher channels is conjectural, but such a device would greatly simplify the instrumentation and would be capable of providing a rough estimate of T_c if it were reasonably accurate.

It is even easier to generate records of temporal fading: The received process corresponding to each phase-stable tone is passed through a bandpass filter and then envelope detected, and the amplitude of the envelope is recorded. Since the physical channel may change rapidly with time for some links, it is appropriate to record simultaneously the envelopes of several independent tones in order to obtain enough data to make a meaningful statistical characterization.

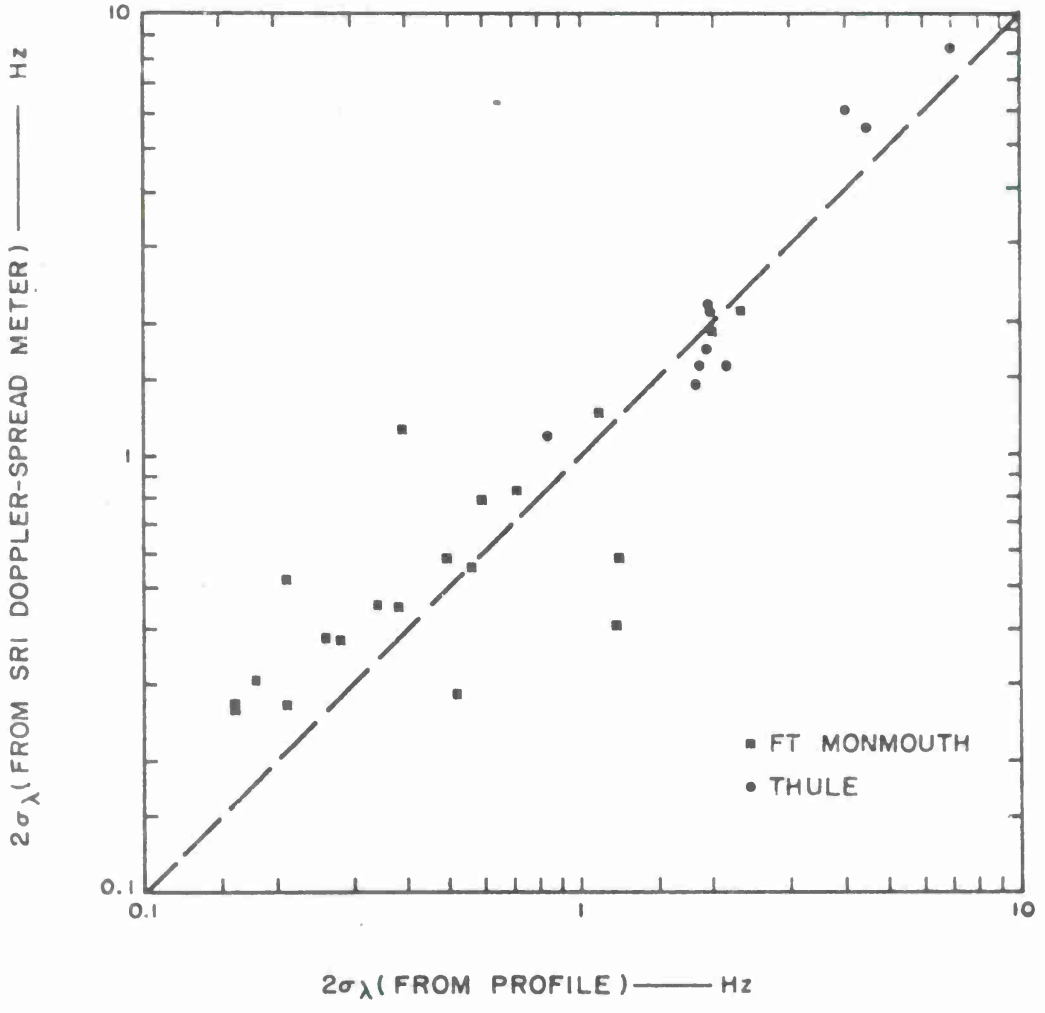

IA-34,658

Figure 4 COMPARISON OF SRI DOPPLER SPREAD METER OUTPUT WITH PROFILE-DERIVED SPREAD

SECTION V

EVALUATION OF BANDLIMITED SIGNALS

Section IV described an experimental program for acquiring data to characterize 10 MHz bandlimited communication channels. The data obtained from the measurements could be used both for signal design and for signal evaluation.

This section describes how the data obtained from the measurements could be used to evaluate the performance of any 10 MHz bandlimited signal that might have been applied to the experimental channel while that channel was being measured. The principal contribution of this section is to present a technique for realizing a device to evaluate arbitrary bandlimited signals. The signal to be evaluated and the experimentally measured time-varying tap-gain functions would be supplied as inputs to the device, and its output would be a representation of the signal that would have been received had it been transmitted over the measured channel. Thus the device could be regarded as a channel playback machine rather than a simulator. However, the device could be used to simulate some effects other than those directly measured. The modification and use of the playback device for simulation is briefly discussed in Section 5.2.

5.1 Realization of a Playback Device

We employ the tap-gain model of a dispersive channel described in Section 2.3 to conceptually guide our development of a channel playback device. Suppose the real, narrowband signals s(t) and r(t) given by (1) and (9) are the channel input and output, respectively. Repeating (1) and (9), we recall that

$$s(t) = \text{Re}\ \{x(t)e^{j2\pi f_o t}\} \tag{44}$$

and

$$r(t) = \text{Re}\{y(t)e^{j2\pi f_o t}\} \tag{45}$$

where x(t) and y(t) are the complex envelopes of the channel input and output, respectively, whose bandwidths are small compared to the carrier frequency f_o. These complex envelopes can be expressed in terms of their real and imaginary components:

$$x(t) = u(t) + j\ v(t) \tag{46}$$

and

$$y(t) = w(t) + j\ z(t) \tag{47}$$

where w(t), z(t), u(t), and v(t) are all real functions. Thus (44) and (45) become

$$s(t) = u(t) \cos 2\pi f_o t - v(t) \sin 2\pi f_o t \tag{48}$$

and

$$r(t) = w(t) \cos 2\pi f_o t - z(t) \sin 2\pi f_o t \tag{49}$$

We now express the complex envelope of the received signal in terms of the tapped delay-line model of the channel. Repeating (18),

$$y(t) = \sum_j m_j(t)\ x\ (t - T_j), \tag{50}$$

where the $\{m_j(t)\}$ are time-varying, complex tap-gain functions with real and imaginary (i.e., "in-phase" and "quadrature") components

$$m_j(t) = m_{Ij}(t) + j\, m_{Qj}(t), \tag{51}$$

where the $\{m_{Ij}(t)\}$ and the $\{m_{Qj}(t)\}$ are real functions.

Combining equations (46), (47), (50), and (51), we obtain

$$w(t) = \sum_j \left[m_{Ij}(t)u(t-T_j) - m_{Qj}(t)v(t-T_j) \right] \tag{52}$$

and

$$z(t) = \sum_j \left[m_{Ij}(t)v(t-T_j) + m_{Qj}(t)u(t-T_j) \right] \tag{53}$$

Equations (48), (49), (52), and (53) suggest the following technique for realizing a playback device:

i. Extract the in-phase and quadrature components u(t) and v(t) from the signal to be evaluated;

ii. Using the experimentally measured tap-gain functions, determine the in-phase and quadrature components w(t) and z(t) of the channel output according to equations (52) and (53);

iii. Finally, form the channel output r(t) from equation (49).

Figure 5 is a block diagramatic representation of the operations to be performed by the playback device.

We now show one way in which the operations illustrated in Figure 5 might be accomplished by hardware. Basically we will extract the in-phase and quadrature components of the channel input as analog signals; we will then convert these signals to digital form and will transmit the digital representations along a tapped shift register to obtain the delayed functions specified in (52) and (53); at each tap, we will supply the appropriate complex tap gain functions provided by the experimental data, will convert both the signal functions and tap-gain functions to

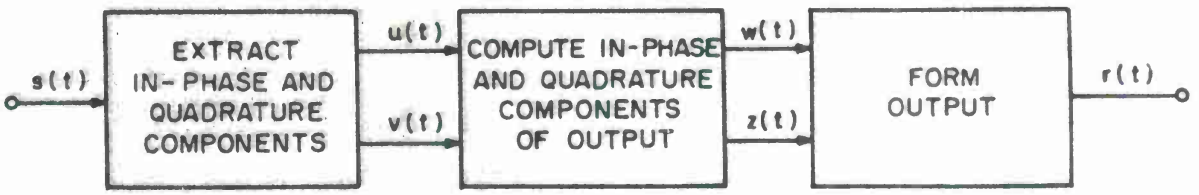

Figure 5 OPERATIONS PERFORMED BY PLAYBACK DEVICE

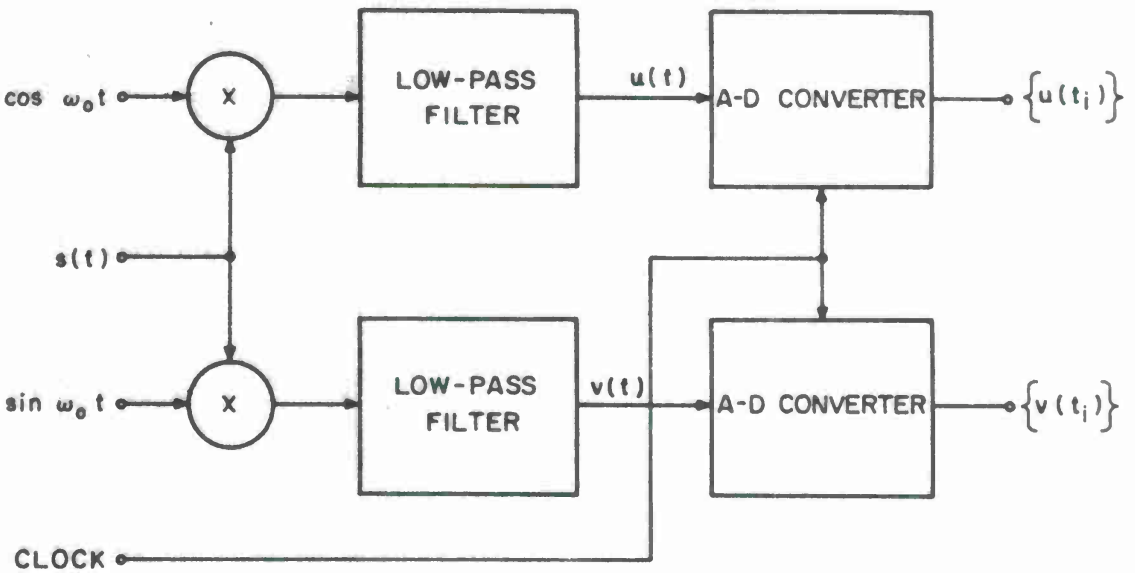

IA-34,659

Figure 6 EXTRACTION OF IN-PHASE AND QUADRATURE COMPONENTS

analog functions, and will perform analog multiplication to compute the individual terms in (52) and (53); the in-phase and quadrature components of the channel output will be computed by analog summations to obtain (52) and (53); and finally the channel output will be provided by (49). Although this realization uses mostly analog hardware to perform the computations, we recognize that it may be possible to use completely digital hardware to calculate the tap outputs and the summations (52) and (53), at which point the time functions w(t) and z(t) would be provided by a digital-to-analog converter. Although the latter, all-digital approach has some attractive features, it would appear that the hybrid technique is somewhat cheaper to implement with current technology.

The in-phase and quadrature components of the channel input could be extracted by the circuit shown diagramatically in Figure 6. The analog-to-digital converters would supply digital representations of these components to a shift register, which would also serve as a delay line. Presently there are A-D converters available that can supply 6-bit samples at a 30 MHz rate, so that at the current level of technology, a channel playback device built on the principles described herein can be used to evaluate in real time signals whose bandwidth does not exceed 15 MHz. This does not imply that it is impossible to build a playback device to evaluate a signal whose bandwidth exceeds 15 MHz; assuming the channel measurements data are suitable to characterize the channel over bandwidths exceeding 15 MHz, the playback device described herein can evaluate the channel effects on signals having higher bandwidths if both the applied signal and the tap-gain data are slowed appropriately.

Figure 7 is a block diagram that shows how the channel output is calculated, given the in-phase and quadrature components of the channel input, and the in-phase and quadrature tap-gain functions ob-

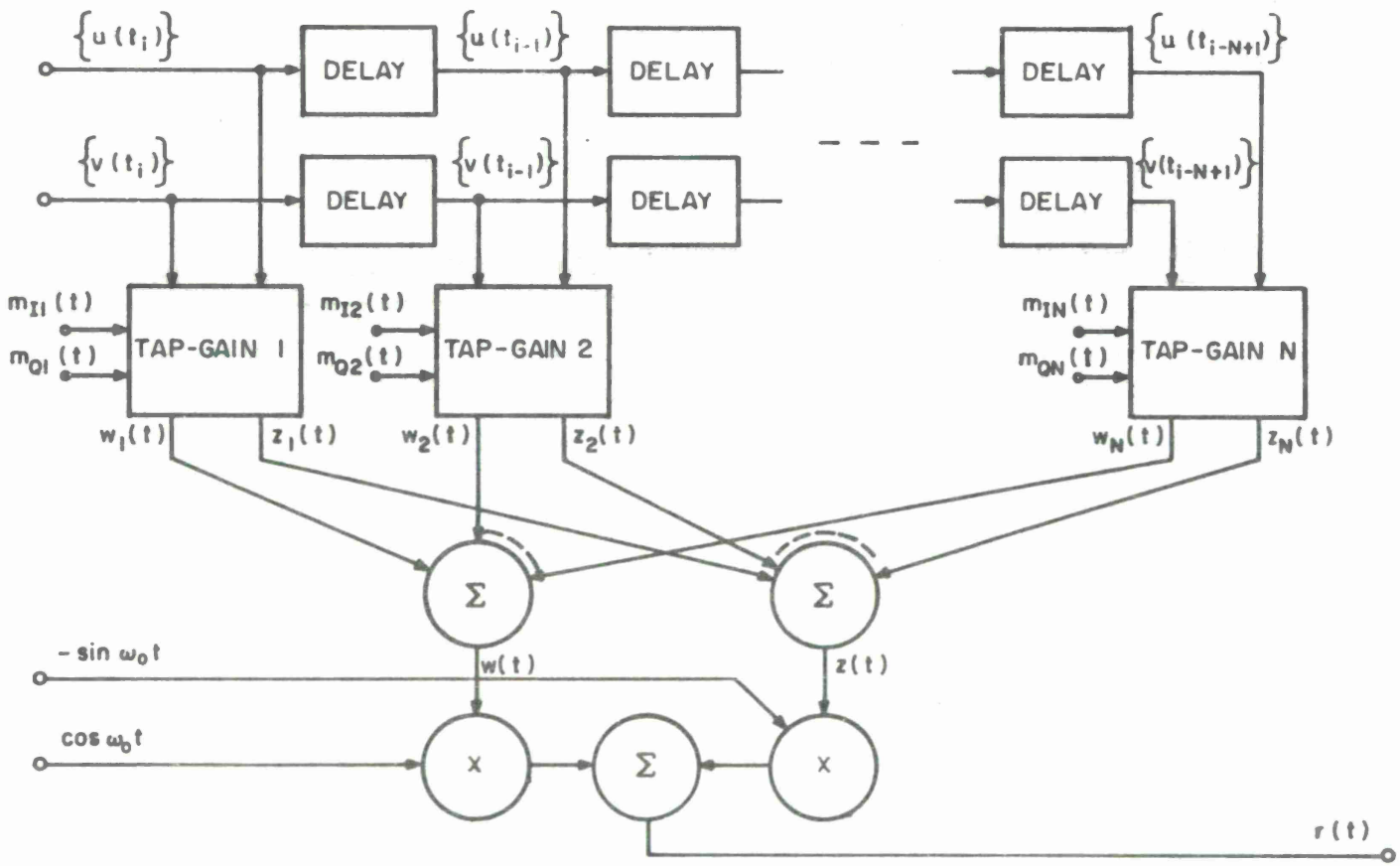

Figure 7 CALCULATION OF CHANNEL OUTPUT

tained from the experimental data. The processing indicated in Figure 7 is essentially independent of whether the equipment is analog, digital, or some hybrid combination. The outputs of the tap-gain calculators are summed to provide the in-phase and quadrature components of the channel output, given by (52) and (53), and then the channel output is determined from (49). The operation of a typical tap-gain calculator is shown in Figure 8. The outputs of the tap-gain calculators are the individual terms appearing in (52) and (53). As we noted earlier, the realization shown here for the tap-gain calculators is essentially analog, while an equivalent all-digital realization could also be shown. We believe that the analog realization is somewhat cheaper than a digital realization at this time, however.

Since the measured phases of both the tap-gain functions $\{m_j(t)\}$ and the baseband signal $x(t)$ are arbitrary in the sense that the received signal is not phase-locked to the transmitted signal, the output of the playback device must be phase insensitive. Specifically this means that if the channel input $s(t)$ given by (44) produces a channel output $r(t)$ given by (45), then the channel input

$$s_\phi(t) = \text{Re}\ \{x(t)e^{j\phi}e^{j2\pi f_o t}\} \tag{54}$$

must produce the corresponding channel output

$$r_\phi(t) = \text{Re}\ \{y(t)e^{j\phi}e^{j2\pi f_o t}\}. \tag{55}$$

In Appendix A we show that the playback device is indeed phase insensitive, which is a requirement for the device to be useable in evaluating the effects of the channel on an arbitrary bandlimited signal $s(t)$.

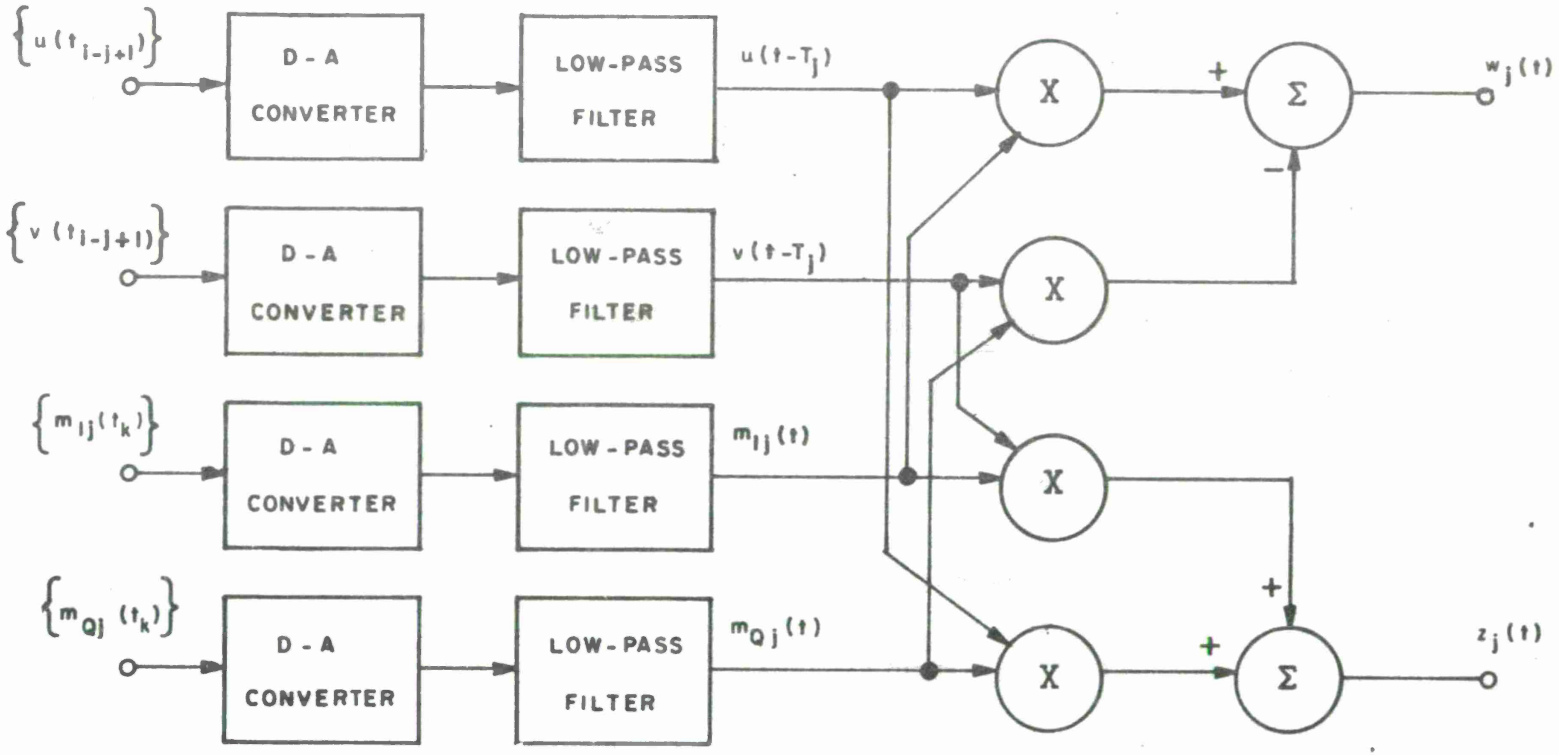

Figure 8. $_j$TH TAP GAIN CALCULATOR

5.2 Simulation Using the Playback Device

Although the device just described is not truly a simulator, since it is only capable of reproducing the effect of the measured channel on an arbitrary bandlimited signal, it can be modified to provide a limited degree of simulation that is appropriate for some practical classes of channels. Two important cases where such a simulation might be useful are the evaluation of ducting effects or of variations in relative terminal geometries that occur on line-of-sight, air-to-air communication links.

Typically, the signal received over such links consists of two components: the direct signal propagated over the line-of-sight path between the two terminals, and a multipath signal consisting of the received signal that is reflected from the ground. In most cases the direct signal is nearly specular -- i.e., its dispersion is nearly zero -- while the reflected signal may be specular, diffuse, or the summation of a diffuse component plus one or more specular reflections.

5.2.1 Simulation of Ducting

When ducting occurs, it turns out that the magnitude of the direct signal is enhanced or attenuated with respect to free-space propagation depending on the location of the terminals with respect to the ducting mechanisms. On the other hand, the magnitude of the reflected signal is likely not to fluctuate because of ducting. If the first few taps of the playback device represent the contributions to the received signal from the direct component, then the effects of ducting can be simulated and thus evaluated in the playback device by varying the gains of the first few taps in a manner that corresponds statistically to the variations in the strength of the direct path arising from ducting phenomena. This simple modification would increase the usefulness of the playback device, provided that the statistical properties of the ducting could be recorded or otherwise accounted for.

5.2.2 Simulation of Variations in Flight Path

It has been suggested that the statistical properties of the reflected component of LOS, A-A links depends quite strongly on the angle of incidence to the specular reflecting point and on the type of terrain over which the aircraft are flying, and except for magnitude, rather weakly on the absolute heights of the aircraft. Of course, the displacement in time and frequency between the direct component and the reflected component of the received signal does depend on the complete terminal geometries and dynamics. These displacements, however, can be easily calculated from knowledge of the terminal geometries and dynamics.

This observation suggests that the playback device can be modified to simulate the behavior of channels that would be encountered on different flight paths than those over which the channel measurements were made. The principal change in the playback device would be to have the taps corresponding to the direct path effectively moved closer to or further from the reflected component of the received signal. For example, suppose that the two aircraft making the channel measurements had each flown at 30,000 feet and were separated by 30 miles, and that the system designer wished to evaluate a channel for two aircraft each flying at 5,000 feet and separated by 5 miles. The original separation between the direct component and the reflected component of the received signal would have been about 11.55 μsec., while the corresponding separation for the channel to be evaluated would be about 1.93 μsec. If the first 15 taps of the playback device correspond to the direct component of the received signal, then the effects of the channel to be evaluated could be approximated by using the original data, but by moving the signal inputs of the first 15 taps of the playback device approximately 9.62 μsec. down the complex digital delay line containing the sampled values of the signal to be evaluated.

The use of the playback device for simulations of ducting and flight path variations would increase its flexibility and usefulness as a tool for evaluating channel effects on bandlimited signals.

SECTION VI

DESIGN OF DIGITAL SIGNALS

This section treats the problem of devising digital signaling techniques that are appropriate for communicating over dispersive channels. The subject encompases both waveform design and signal processing. Section 6.1 indicates how the channel characteristics listed in Section 4.1.1, which would be provided as data outputs of the experimental program described in Section IV, might influence the specification of modulation, coding, and diversity techniques. Section 6.2 discusses other factors that may have to be considered in the design of signals. Section 6.3 indicates roughly the best performance that can be attained for digital signaling over a large class of dispersive channels, and it demonstrates how to design signals for those channels that nearly reach the optimum level of performance.

6.1 Channel Influences on Signal Design

The problem of designing a signaling technique consists of specifying particular modulation, detection, error control, and diversity techniques. In this section we examine the ways in which the channel characteristics listed in Section 4.1.1 influence the specification of each of these various techniques.

6.1.1 Channel Influences on Specifying Modulation

Throughout the remainder of this section, we restrict our attention to the design or analysis of digital signals that belong to the following general class: The symbol waveform that represents a message symbol selected from some q-ary alphabet, $q \geq 2$, consists of the sequential transmission of n T-second chip waveforms for some $n \geq 1$. Each chip waveform consists of the simultaneous transmission of m phase-stable tones for some $m \geq 1$. Hence each q-ary symbol is represented by a n-chip symbol waveform whose time-frequency-phase

pattern is distinct from the symbol waveforms used to represent each of the remaining q-1 message symbols. This class of waveforms includes many commonly used digital modulation techniques, such as binary and M-ary FSK, binary and M-ary PSK, hybrid FSK/PSK combinations, frequency-hopping (FH) signals, and pseudo-noise phase-modulated (PN) signals.

Given this class of admissable waveforms, we examine what effects the channel characteristics might exert on selecting the chip period, the number of chips per symbol, the frequency separation between tones, the power margin, the required interval between successive transmissions on a given frequency, and the use of coherent or incoherent detection techniques.

The essential meaning of the coherence bandwidth is that it indicates roughly the frequency separation necessary for the fading of two tones to be independent. This parameter would influence the design of signal waveforms in a number of ways. For transmitted - reference PSK systems or frequency - differentially coherent PSK systems (like ANDEFT [7]), the data tones and reference tones would have to be located in a bandwidth somewhat less than the coherence bandwidth of the channel. On the other hand, for some multitone, coded systems or FH systems in which it is intended that the fading on each tone be independent, the frequency separation between adjacent or different tones ought to be somewhat greater than the coherence bandwidth of the channel. For bandlimited signals this would equivalently place an upper bound on m, the number of independent tones that could be transmitted per chip, or on n, the number of independently fading chips that could be transmitted in a FH sequence.

The major way in which the coherence time would influence waveform design is that is would set an upper bound on the chip duration T if coherent or differentially coherent detection is to be used. This

consideration is especially important in the design of PSK systems where the phase, and not the energy, of the signal is determined by the the modulator. A very short coherence time might prohibit the use of PSK.

Both the temporal and the spectral statistical characterizations of fading would provide indications of the power margin required to attain a given performance; two channels with similar coherence times and bandwidths could have fades whose depths were characterized by considerably different probability distributions. Of course, if diversity techniques could be profitably employed, the power margin could be reduced accordingly. The spectral characterization of fading would provide an indication of the ability to usefully employ frequency diversity either explicitly, or within the signal structure as in, for example, a wideband FH signal.

The time-delay profile could influence waveform design in several ways. On line-of-sight channels characterized by a direct path followed by a reflected signal component, it might be possible to choose the chip period T to be shorter than the delay between the direct and reflected components. This technique would be effective in removing entirely the effects of multipath propagation, provided the reflected signal can be fully rejected in the adjacent chip. On the other hand, it might be preferable to design a signal whose chip period is much greater than the maximum time spread between significant channel reflections. For the class of allowable waveforms, this would ensure that for most of the chip period, the received signal would be an undistorted, although attenuated and phase-shifted, version of the transmitted signal[8]. The maximum time spread between significant channel reflections would also provide a lower bound to the intervals between successive uses of the same frequency in a FH system. Finally, the characterization of the time-delay profile could indicate the accuracy

to which received signals could be used to make time-of-arrival measurements.

6.1.2 Channel Influences on Error Control Techniques

By supplying the modulator not only with message symbols, but also additional, redundant symbols which are algebraically related to the message symbols, it is possible to devise mathematical techniques for detecting and correcting symbol errors that appear at the output of the demodulator. This process is usually called coding. Many coding techniques work well only if the symbol errors supplied to the decoder appear to occur statistically independently of one another. There are, however, many known classes of burst-error-correcting codes which work well on channels in which decoding errors occur in bursts, provided that the burst lengths are sufficiently short and that the error-free intervals, or "guard spaces", between successive bursts of errors are sufficiently long. Independent-error-correcting codes can also be applied to burst-error channels, however, if a suitable interleaver is used to separate the bursty errors and thus to make the errors supplied to the decoder appear to occur independently. The use of coding and interleaving to correct demodulation errors is also called error control.

It is well beyond the scope of this report to discuss error control techniques in any detail. Coding is treated exhaustively in the books by Peterson [9] and by Berlekamp [10] and in an excellent but unpublished report by Forney [11]. Ramsey [12] has described a class of techniques for efficiently constructing interleavers.

In general, two parameters determine the effectiveness of an independent-error-correcting code: the normalized information rate (or "rate"), which is the ratio of information symbols to total symbols transmitted over the channel; and the constraint length of the code, which essentially indicates the number of contiguous channel symbols

whose selection is influenced by any information symbol. The maximum allowable rate depends on the decoding error probabilities; of course, as the decoder makes more errors, the rate must be decreased sufficiently so that the additional fractional redundancy may be used to mathematically detect and correct the fractionally more probable errors. Section 6.1.1 described some of the ways in which a dispersive channel might influence signal design in order to reduce decoding errors. Except for those considerations, the channel has relatively little influence in determining the coding rate. For codes with a given rate, the decoding error probability tends to decrease exponentially with the constraint length, while the decoding complexity tends to increase exponentially. The choice of a constraint length depends mostly on the system designer's willingness to trade complexity for performance, and is hardly influenced by the characteristics of the channel.

For burst-error-correcting codes, the channel parameters exert considerably more influence in the choice of code parameters. Codes can be designed to correct all bursts of errors in which the errors occur within a contiguous span of L channel symbols, provided all bursts are separated by an error-free "guard space" of G contiguous channel symbols, and provided further that $G/L \geq 3$. Furthermore, this class of errors is usually the only class of errors the code can correct, and therefore it is essential that the code be matched as closely as possible to the statistical properties of the decoding errors. In particular, L should be made as large as possible in order to accommodate long error bursts, while G should be made as small as possible in order to correct closely spaced bursts. Bursts whose lengths exceed L or whose guard spaces are less than G will cause decoding errors; it is exceedingly difficult to find a value for L that efficiently matches the channel statistics. Of course, the coherence time influences the selection of L, since it indicates the

time span over which decoding errors are correlated.

Another technique for correcting errors on a burst error channel is to use an interleaver to make the channel errors appear to occur independently, and then to apply a suitable independent-error-correcting code to the output of the interleaver. The system designer can specify a (n_2,n_1) interleaver, which reorders a sequence in such a way that no contiguous sequence of n_2 symbols in the reordered sequence contains any symbols that were separated by fewer than n_1 symbols in the original ordering [12]. Thus n_2 must be greater than or equal to the constraint length of the code, while n_1 must be chosen to be larger than any burst length to be expected in the decoded sequence. The choice of n_1 and n_2 is not critical, provided they are sufficiently large; there is no tradeoff or "matching" required as in the case of a burst-error-correcting code. The principal way in which the channel influences the selection of n_1 is that the coherence time can be used to set a lower bound on n_1; the selection of n_2 depends only on the constraint length of the code, and is unaffected by the channel characteristics.

6.1.3 Channel Influences on Using Diversity Combining Techniques

Here we consider only "explicit" diversity combining techniques, such as frequency diversity and space diversity, in which the receiver combines in some appropriate manner the signals obtained from two or more hopefully independent replicas of the transmitted signal prior to detection. It is again beyond the scope of this report to treat diversity combining techniques in detail; this was accomplished some time ago by Brennan [13]. It is sufficient to observe that the performance advantage to be gained by using diversity depends mostly on the order of diversity D, which is the number of independent diversity signals that are combined in the receiver.

For frequency-diversity systems, D identical baseband signals are simultaneously transmitted at D carrier frequencies, and the

carriers are separated sufficiently so that there is no spectral overlap between the various diversity signals. From Section 6.1.1, it is evident that the effectiveness of using frequency diversity depends on the coherence bandwidth and the spectral fading characteristics of the channel. The coherence bandwidth imposes an upper bound on D if the composite signal is to be bandlimited, or equivalently, it sets a lower bound on the frequency separation between adjacent diversity signals.

Space-diversity systems employ D spatially-distributed antennas to hopefully receive independently distorted versions of the transmitted signal. Space diversity is most effective when the reflected signal is diffuse rather than specular. An examination of the time-delay profile would reveal whether the channel reflections appear to be predominantly diffuse or specular, and would therefore provide an indication to the system designer as to the effectiveness of using space diversity.

6.2 External Factors Influencing Signal Design

The preceding discussion has assumed that the system designer is free to design a signal format that is compatible with the class of channels over which he intends to communicate, and furthermore that the channel corruption is the only factor for which he will have to compensate. In practice, of course, neither of these assumptions may be true. The designer, for example, may be severely limited in his choice of signaling techniques by economic considerations. Conversely, in some applications such as jam-proof military communication systems, the external conditions imposed on the signal capability may be so stringent that almost any signaling technique that satisfies the external conditions could provide reliable communication over the fading channels. While the consideration of these external factors is largely beyond the scope of this report, it is important to point out that in

practice it may be these factors rather than propagation characteristics that are most influential in guiding signal design.

A few of the more obvious or common external limitations are the following: The transmitter may be power-limited. This is especially true in airborne or spacecraft links. The receiver may not be able to employ space diversity, because there might be no available location to install a second receiving antenna. The communicators may be unable to secure a bandwidth allocation from the appropriate governmental regulatory body that is sufficiently large to accommodate the most effective signaling structures for communicating over the channel. Finally, some applications might be required to meet the needs of a large number of budget-limited users, so that the signal designer would be required to specify some well-known, relatively inexpensive signaling technique like binary FSK or like binary or quarternary DPSK. In this case the system designer might only be allowed to specify the chip period T. For FDM systems, for example, he might then be able to apply the methods outlined by Bello and Nelin [14] to optimize T, where the optimal value of T is a compromise between being small to combat time-selective fading and being large to combat frequency-selective fading.

6.3 Signal Design and Performance for a Class of Dispersive Channels

Here we summarize some results due to Kennedy and Lebow[15] that suggest design techniques and indicate attainable performance levels for digital communication over dispersive channels in which the received signal is essentially a one-component signal that is scattered diffusely about some mean time delay and Doppler shift. Typical channels for which this condition holds include HF and tropo-scatter channels. The time-delay spread and the Doppler spread of the channel are σ_τ and σ_λ, respectively. Using the approximations (38) and (39), the coherence bandwidth of the channel is approximately equal to the reciprocal of the time-delay spread and the coherence

time is approximately equal to the reciprocal of the Doppler spread.

The fundamental approach used by Kennedy and Lebow to analyze the performance of digital modulation techniques is to plot the time-frequency occupancy of a chip on a two-dimensional grid whose temporal spacing is equal to the coherence time of the channel and whose frequency spacing is equal to the coherence bandwidth of the channel. The number of grid rectangles occupied by a chip, z, is termed the diversity per chip, and it represents physically the approximate number of independent fading component contained in the signal used to transmit a chip. They then indicate an approximate expression for the binary error probability of a signal consisting of n chips whose total received signal energy in all n chips is E, being received by a receiver whose noise power density in N_o watts/H_z. This expression, which approximates the results obtained by several investigators, is the following [15]:

$$P(E) \cong 0.2 \exp -\tfrac{1}{2} A(y)(E/N_o), \tag{56}$$

where

$$y = \frac{zn}{E/N_o}, \tag{57}$$

and A(y) is an "efficiency" whose value is plotted in Figure 9. Figure 10 is a graph of Equation (56), the probability of error curve.

Kennedy and Lebow then show how the preceding results can be applied to the design of efficient digital signals. First, Figure 9 indicates that the efficiency A(y) has a broad maximum of about 0.3 centered approximately at y = 0.35. This suggests that the optimum value of y corresponds to

$$\frac{1}{y} = \frac{E/N_o}{zn} \cong 3, \tag{58}$$

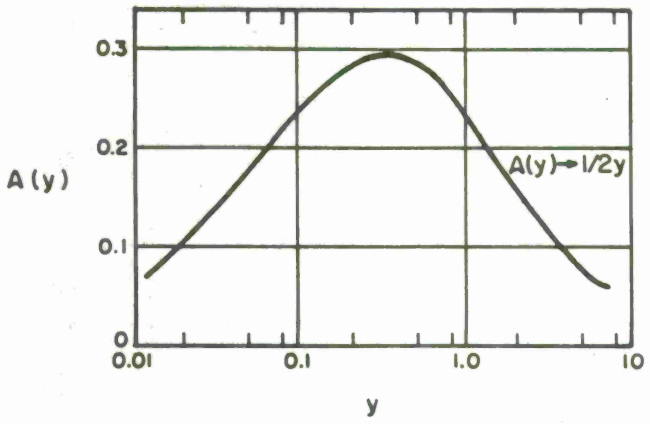

Figure 9 THE EFFICIENCY A(y)

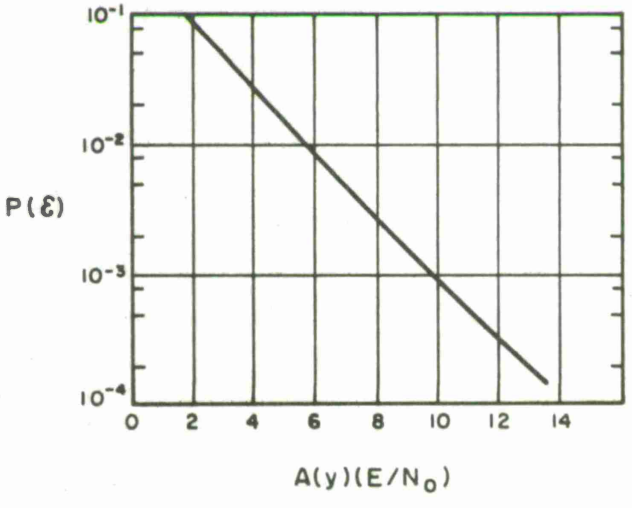

IA-34,718

Figure 10 ERROR PROBABILITY

or effectively that the signal to noise ratio per diversity element should be 3 for the most efficient use of the signal power.

To illustrate the application of these results to the design of signals, consider a channel for which $\sigma_\tau = 1$ μs and $\sigma_\lambda = 10$ Hz, corresponding to a channel coherence bandwidth of 1 MHz and a channel coherence time of 0.1 second. Suppose that $P(E) = 10^{-3}$ is a design goal. From Figure 10, $A(y)(E/N_o) \cong 10$. The most efficient performance occurs when $y \cong 0.35$ or $A(y) \cong 0.3$; in this case

$$E/N_o \cong \frac{10}{0.3} = 33.3 \tag{59}$$

Equation (59) now defines the signal energy that must be transmitted using the most efficient signal structure to achieve a decoding error probability of 10^{-3}. To achieve this, we must have

$$zn = \frac{E/N_o}{3} = \frac{33.3}{3} \cong 11, \tag{60}$$

or we need 11 diversity elements. For a non-bandlimited channel, one possible solution to the signal design problem would be to use an 11-chip FH signal, where the separation between different tones would be at least 1 MHz due to the coherence bandwidth of the channel.

The signal designed in the preceding example required an RF bandwidth of approximately 10 MHz to attain sufficient diversity in the signaling structure to make the most efficient use of the transmitted power. Let us now consider the case where the channel is bandlimited. Suppose, for example, the channel has a bandwidth of 5 MHz, or effectively 5 diversity elements available in the frequency domain. Rewriting (57),

$$zn = 5 = y(E/N_o) \tag{61}$$

while Figure 10 indicates, as before, that

$$A(y)(E/N_o) \cong 10. \tag{62}$$

Simultaneous solution of (61) and (62) yields the parametric equation

$$A(y) = 2y, \tag{63}$$

the solution of which is $A(y) \cong 0.25$ from Figure 9. Substituting $A(y) = 0.25$ in (62), we obtain the solution $E/N_o = 40$ for the band-limited case, indicating that for this example the effect of band-limiting the channel costs about 1 dB of signal energy to attain the same error probability as for the non-bandlimited case.

For $A(y) = 0.3$, the optimum value, (56) reduces to

$$P(E) \cong 0.2 \exp - 0.15\ E/N_o. \tag{64}$$

For the nondispersive Gaussian channel, on the other hand,

$$P(E) \cong k \exp - 0.5\ E/N_o. \tag{65}$$

Thus for binary signaling, a dispersive channel requires at least 5 dB more energy per signaling element than is required for a non-dispersive channel to attain a given error probability. Kennedy and Lebow show that as the symbol alphabet size is increased, this apparent difference between dispersive and nondispersive channels can be reduced artibrarily. This topic, however, is beyond the scope of this report.

APPENDIX A

PROOF THAT THE CHANNEL PLAYBACK DEVICE IS PHASE INSENSITIVE

We asserted that the channel playback device described in Section V is phase insensitive. This means that if the channel input

$$s(t) = \text{Re}\{x(t)e^{j2\pi f_o t}\} \tag{A-1}$$

produces the channel output

$$r(t) = \text{Re}\{y(t)e^{j2\pi f_o t}\}, \tag{A-2}$$

then the channel input

$$s_\phi(t) = \text{Re}\{x(t)e^{j\phi}e^{j2\pi f_o t}\} \tag{A-3}$$

must produce the channel output

$$r_\phi(t) = \text{Re}\{y(t)e^{j\phi}e^{j2\pi f_o t}\}. \tag{A-4}$$

We prove that assertion in this Appendix.

Since

$$x(t) = u(t) + j\,v(t) \tag{A-5}$$

and

$$y(t) = w(t) + j\,z(t), \tag{A-6}$$

then

$$\text{Re } \{x_\phi(t)\} = \text{Re } \{x(t)e^{j\phi}\}$$

$$= u(t) \cos \phi - v(t) \sin \phi \qquad \text{(A-7)}$$

and

$$\text{Im } \{x_\phi(t)\} = u(t) \sin \phi + v(t) \cos \phi \ . \qquad \text{(A-8)}$$

To show that the input $s_\phi(t)$ produces the output $r_\phi(t)$, it is sufficient to show that

$$\text{Re } \{y_\phi(t)\} = \text{Re } \{y(t)e^{j\phi}\}$$

$$= w(t) \cos \phi - z(t) \sin \phi, \qquad \text{(A-9)}$$

and

$$\text{Im } \{y_\phi(t)\} = w(t) \sin \phi + z(t) \cos \phi. \qquad \text{(A-10)}$$

By using the channel playback device, we obtain from equation (52)

$$\text{Re } \{y_\phi(t)\} = \sum_j \Big[m_{Ij}(t) \text{ Re } \{x_\phi(t-T_j)\} - m_{Qj}(t) \text{ Im } \{x_\phi(t-T_j)\} \Big] \qquad \text{(A-11)}$$

Using (A-7), (A-8), (52), and (53), (A-11) becomes

$$\begin{aligned}
\text{Re}\{y_\phi(t)\} &= \sum_j \Big\{ m_{Ij}(t)\left[u(t-T_j)\cos\phi - v(t-T_j)\sin\phi\right] \\
&\quad - m_{Qj}(t)\left[u(t-T_j)\sin\phi + v(t-T_j)\cos\phi\right]\Big\} \\
&= \cos\phi \sum_j \left[m_{Ij}(t)\,u(t-T_j) - m_{Qj}(t)\,v(t-T_j)\right] \\
&\quad - \sin\phi \sum_j \left[m_{Ij}(t)\,v(t-T_j) + m_{Qj}(t)\,u(t-T_j)\right] \\
&= w(t)\cos\phi - z(t)\sin\phi. \qquad \text{(A-12)}
\end{aligned}$$

This establishes (A-9). A similar computation establishes (A-10), and the assertion is proved.

This page left Intentionally blank

REFERENCES

1. J. M. Wozencraft and I. M. Jacobs, Principles of Communication Engineering, Wiley, New York, N.Y., 1965.

2. R. F. Daly, "Analysis of Multipath Effects on FSK Error Probability for a Simple HF Channel Model", Research Memo 1, Contract SD-189, Stanford Research Institute, Menlo Park, California, February, 1964, AD-816 288.

3. R. S. Kennedy, Fading Dispersive Communication Channels, Wiley, New York, N.Y., 1969.

4. R. F. Daly, "A Power Spectrum Program for Estimating the Doppler Profile of a Radio Channel", Res. Memo 15, Contract DA36-039 SC-87197, Stanford Research Institute, Menlo Park, California, October, 1964, AD 613 195.

5. S. O. Rice, "Statistical Properties of a Sine Wave Plus Random Noise", Bell Syst. Tech. J., 27, pp. 109-157, 1948.

6. R. T. Wolfram, K. D. Felperin, and B. C. Topper, "SRI Doppler Spread Meter", Stanford Research Institute, Menlo Park, California, December, 1965.

7. G. C. Porter, M. B. Gray, and C. E. Perkett, "A Frequency-Differential Phase-Shift Keyed Digital Data Modem for Operation at 4800, 2400, 1200, and 600 Bits Per Second Over Long-Range HF Paths", ESD-TR-66-639, General Dynamics, Electronics Division, Rochester, New York, October, 1966, AD-650 726.

8. P. A. Bello, "Selection of Multichannel Digital Data Systems for Troposcatter Channels", IEEE Trans., COM-17, pp. 138-161, April, 1969.

9. W. W. Peterson, Error-Correcting Codes, M.I.T. Press, Cambridge, Massachusetts, 1961.

10. E. R. Berlekamp, Algebraic Coding Theory, McGraw-Hill, New York, N.Y., 1968.

11. G. D. Forney, Jr., "Coding System Design for Advanced Solar Missions", Final Report, Contract NAS2-3637, Codex Corporation, Watertown, Massachusetts, December, 1967, N68-16388.

12. J. L. Ramsey, "Realization of Optimum Interleavers", IEEE Trans., IT-16, pp. 338-345, May, 1970.

13. D. G. Brennan, "Linear Diversity Combining Techniques", Proc. IRE, 47, pp. 1075-1102, June, 1959.

14. P. A. Bello and B. D. Nelin, "Optimization of Subchannel Data Rate in FDM-SSB Transmission Over Selectively Fading Media", IEEE Trans., COM 12, pp. 46-53, March, 1964.

15. R. S. Kennedy and I. L. Lebow, "Signal Design for Dispersive Channels", IEEE Spectrum, pp. 231-237, March, 1964.

Security Classification

DOCUMENT CONTROL DATA - R & D

(Security classification of title, body of abstract and indexing annotation must be entered when the overall report is classified)

1. ORIGINATING ACTIVITY (Corporate author)	2a. REPORT SECURITY CLASSIFICATION
The MITRE Corporation P.O. Box 208 Bedford, Massachusetts	Unclassified
	2b. GROUP

3. REPORT TITLE

Characterization and Measurement of Dispersive Channels

4. DESCRIPTIVE NOTES (Type of report and inclusive dates)

5. AUTHOR(S) (First name, middle initial, last name)

John L. Ramsey

6. REPORT DATE	7a. TOTAL NO. OF PAGES	7b. NO. OF REFS
NOVEMBER 1971	62	15

8a. CONTRACT OR GRANT NO.	9a. ORIGINATOR'S REPORT NUMBER(S)
F19(628)-71-C-0002	ESD-TR-71-382
b. PROJECT NO. 511A	
c.	9b. OTHER REPORT NO(S) (Any other numbers that may be assigned this report)
d.	MTR-2184

10. DISTRIBUTION STATEMENT

Approved for public release; distribution unlimited.

11. SUPPLEMENTARY NOTES	12. SPONSORING MILITARY ACTIVITY
	Electronic Systems Division, Air Force Systems Command, L. G. Hanscom Field, Bedford, Massachusetts 01730

13. ABSTRACT

This report is concerned with the characterization and study of dispersive channels. It shows how and why the physical channel distorts signals, it presents an experimental program for acquiring data to characterize the channel, and it indicates how the experimental data could be used either to evaluate the performance of arbitrary signaling techniques or to design effective signals for communicating over the channel.

DD FORM 1 NOV 65 1473

Security Classification

14. KEY WORDS	LINK A		LINK B		LINK C	
	ROLE	WT	ROLE	WT	ROLE	WT
DISPERSIVE CHANNELS						
SIGNAL DISTORTION						
PROPAGATION						